Memorias de SICEL 2023 | UNIVERSIDAD NACIONAL DE COLOMBIA

Estrategia de Control Secundario sin Comunicaciones para Microrredes Aisladas Desbalanceadas

Secondary Control Strategy without Communications for Unbalanced Isolated Microgrids

Andres Mauricio Salinas-Cala [1A], Juan Manuel Rey-López [1B], María Alejandra Mantilla-Villalobos [1C]

[1]Grupo de investigación en Sistemas de Energía Eléctrica, Escuela de Ingenierías Eléctrica, Electrónica y de Telecomunicaciones, Universidad Industrial de Santander, Colombia. Orcid: 0000-0001-5277-505X[A], 0000-0002-5465-4769[B], 0000-0002-8388-3886[C]. correos electrónicos: andres2218078@correo.uis.edu.co[A], juanmrey@uis.edu.co[B], marialem@uis.edu.co[C]

Recibido: 08/07/2023. Aceptado: 22/08/2023. Versión final: 27/09/2023

Resumen

En el contexto de la transición energética, las microrredes eléctricas se han convertido en una solución para la electrificación de zonas aisladas. En este tipo de aplicaciones, se suelen implementar redes de baja tensión con cargas desbalanceadas. No obstante, la mayoría de las estrategias de control jerárquico presentadas en la literatura, han sido diseñadas para operar ante la presencia de cargas balanceadas. Por esta razón, es relevante estudiar cómo las estrategias de control pueden adaptarse a este escenario, especialmente aquellas que reducen la dependencia de los sistemas de comunicaciones, con el objetivo de mejorar la flexibilidad y confiabilidad. Este trabajo presenta una estrategia de control secundario que no requiere el uso de comunicaciones para operar en microrredes aisladas con cargas desbalanceadas. La estrategia garantiza una adecuada compartición de la potencia entre los generadores distribuidos que componen la microrred. Se presentan resultados de simulación en Matlab/Simulink para validar la estrategia propuesta.

Palabras clave: control secundario; control jerárquico; control descentralizado; microrredes aisladas; cargas desbalanceadas; regulación de frecuencia; generación distribuida; reparto de potencia; componentes simétricas; potencia reactiva negativa.

Abstract

In the context of the energy transition, electrical microgrids have become a key energy solution for isolated zones. For this type of application, low-voltage networks with unbalanced loads are commonly connected. Despite this, many of

How to cite: A. Salinas-Cala, J. M. Rey, M. Mantilla-Villalobos, "Secondary Control Strategy without Communications for Unbalanced Isolated Microgrids," in *XI Simposio Internacional de Calidad de la Energía Eléctrica*, Valledupar: Universidad Nacional de Colombia, Nov. 2023. doi: https://doi.org/10.15446/sicel.v11.110009

the hierarchical control strategies presented in the literature have been designed to operate properly only in the presence of balanced loads. For this reason, it is relevant to study how control strategies can be adapted to this scenario, especially those that reduce the dependence on communications to enhance flexibility and reliability. In this sense, this paper presents a secondary layer control strategy that does not require the use of communications to operate in isolated microgrids with unbalanced loads. The strategy guarantees proper performance in terms of power-sharing between the distributed generators of the microgrid. Simulations on Matlab/Simulink are presented to validate the response of proposal.

Keywords: secondary control; hierarchical control; decentralized control; isolated microgrids; unbalanced loads; frequency regulation; distributed generation; power-sharing; symmetrical components; negative reactive power.

1. Introduction

The world is undergoing an energy transition in which governments and academia are looking for solutions to replace fossil fuel-based energy sources with less polluting technologies, including renewable energy systems [1]. Microgrids (MG) are small-scale electrical systems that operate coordinately distributed generators (DGs) and energy storage technologies to supply local loads [2]. In the energy transition context, electrical microgrids play a strategic role, facilitating the integration of DGs into electrical power systems at the distribution level [3-6].

Microgrids can operate in grid-connected mode or islanded mode. The transition between operation modes improves the reliability of the service provided to users since it allows the segmentation of distribution networks in the event of failures [7,8]. However, due to the long distances to grid connection points and topographic characteristics of the terrain, in some rural remote zones, it is cost-effective to implement autonomous microgrids designed to operate permanently isolated [9,10].

The design of control strategies for isolated microgrids must guarantee a reliable and safe operation with a permanent power supply [11,12]. The most common scheme to implement the operative functionalities of the microgrids is the three-layer hierarchical control presented in figure 1, in which the strategies are associated with layers according to the time scales and control objectives. An important aspect that must be considered when designing control strategies for microgrids is the communication system. Depending on the communication scheme, the strategies can be classified as centralized, distributed or with no communications [13]. As their names suggest, the first two categories require a communication system to exchange data between the controllers of the DGs, making the operation vulnerable to failures due to real-time data transmission issues, which can affect the achievement of the control objectives [14,15]. Considering this aspect, strategies with no communications have emerged as an alternative to reduce the dependence on communication systems and improve reliability [16].

Regarding the secondary layer, the most common strategies to operate without communications are based on low-pass filters [17-19]. These types of proposals offer a design tradeoff between transient response and accuracy. Specifically, if a fast transient response is set, the frequency restoration presents poor performance. On the contrary, a good restoration of the frequency is only achieved if a slow transient response is set. Aiming to improve these limited static and dynamic properties, in [20] and [21], controls with no communications have been proposed based on a scheme that switches between two configurations driven by a time-dependent protocol.

Ideally, the electrical systems are balanced when the loads connected in their phases are identical. However, for isolated applications, the connected loads are mostly single-phase, causing imbalances. In isolated electrical microgrids, this situation can generate power supply problems such as: 1) inappropriate power-sharing between DGs [22]; and 2) active power oscillation due to negative sequence currents. Despite this, many of the hierarchical control strategies presented in the literature have been designed to operate properly only with a balanced load. This is the case of [20] and [21], in which only balanced charges were considered.

This paper presents a control strategy without communications for the secondary layer of isolated microgrids with unbalanced resistive loads. This proposal takes as its starting point the strategies presented in [20] and [21], and maintaining its operational advantages, adapts the scheme to ensure good operational performance in the presence of unbalanced resistive loads in terms of the power-sharing of the DGs. For this purpose, an adaptation of a $Q^- - Z$ control block inspired by the work presented in [23] is proposed. The strategy adds a signal to the primary control, eliminating the mismatches in the power-sharing between DGs through a negative sequence virtual impedance. The proposal is characterized by its simplicity and effectiveness without requiring communication.

This paper is organized as follows: in Section 2 concepts about hierarchical control focused on the secondary layer are presented. Then, in Section 3 the proposed control block is described. Section 4 presents simulations

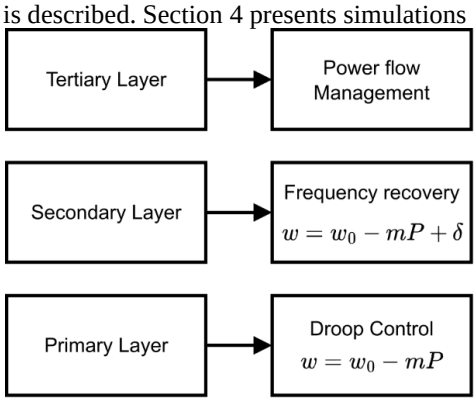

Figure 1. General scheme of a three-layer hierarchical control. Source: elaborated by the authors.

to verify the operation of the proposal. Finally, Section 5 concludes the main remarks.

2. Hierarchical Control for Islanded Microgrids

This section presents key concepts about hierarchical control and describes the base strategy for the secondary layer without communications that will be adapted to operate in the presence of unbalanced loads.

2.1. Operation of islanded microgrids

The bibliography on control strategies for microgrids is extensive and addresses strategies for connected mode, islanded mode, and transition between modes [24,25]. However, there is a clear and widespread tendency to organize control strategies in hierarchical structures [26,27]. The primary layer is usually based on the well-known droop method [28]. This strategy produces a virtual inertia through the emulation of the synchronous generators' operation, allowing distributed generators to achieve a common frequency, which produces the proportional generation of the steady-state powers. However, this method requires the introduction of a deviation in the frequency of operation, which should be restored in the secondary layer [29]. Finally, the tertiary layer acts to control the power flow management of the distributed generators [30,31]. Figure 1 presents a general scheme of a three-layer hierarchical control.

As previously mentioned, the hierarchical layers divide the strategies according to the operational dynamics, so it is possible to decouple the design and analysis of each of its layers [32]. The interest of this work is to analyze the operation of the primary and secondary layers. The findings presented can be generalized to operate in conjunction with different tertiary layer strategies.

The use of communication systems is also fundamental in the way hierarchical control operates in isolated microgrids. The strategies can be classified into three configurations: centralized, distributed, or without communications [33]. In the first category, the strategies are governed by a microgrid central controller (MGCC). The DG controllers send measured signals to the MGCC, which receives and manages the information. The MGCC performs calculations and sends back control signals to the DGs periodically. In the second category, the strategies operate distributed, so the MGCC is not required since the control system is designed to rely on the data interchange between the DGs. These categories have in common the use of communication systems for their operation, making them vulnerable to communication issues such as link failures, data transmission delays, and noise disturbances, among others [14,15]. Although in the second case, reliability improves since it does not depend on the correct functioning of a single equipment (the MGCC), the complexity of installation can increase when numerous DGs are connected. For these reasons, the third category has emerged, in which decentralized control strategies that do not use communication systems are proposed [16]. These types of strategies eliminate the risk of operational failures due to communication issues, although these do not avoid the need to implement a MGCC for other functions such as the DGs coordination during the black start process. Since fewer control layers and operational actions rely on the MGCC performance, the MG will be more reliable [34].

2.2. Secondary layer without communications

The droop control can be defining in equation 1 for frequency regulation as follows

$$\omega = \omega_0 - mP, \tag{1}$$

where the frequency ω rely on the active power P, ω_0 and m are frequency reference and droop control gain, respectively. Active power P corresponds to the instantaneous active power p filtered using a low-pass filter with a cutoff frequency ω_c such as equation 2 to achieve high power-quality injection

$$P(s) = \frac{\omega_c}{s + \omega_c} p(s), \tag{2}$$

where, $P(s)$ and $p(s)$ are Laplace transform of P and p, respectively.

This general definition of droop control is decentralized as it operates exclusively using the local measurements (p and ω). The error in the operating frequency

concerning the reference ω_0 can be recovered by the secondary layer, adding an extra term δ as follows

$$\omega = \omega_0 - mP + \delta. \quad (3)$$

According to how the delta term is calculated, the secondary layer is classified.
The decentralized proposal presented in [20] defines δ as

$$\delta(t) = k_i \int \left[(\omega_0 - \omega(t))\mathrm{sgn}(k(t)) - k(t)\delta(t)\right] dt \quad (4)$$

where k_i is a constant parameter and $k(t)$ is a control parameter driven by a time protocol (sgn corresponds to the sign function or signum function). This time-domain expression can be analyzed in the frequency domain as a switching control with two operation modes: a filtered proportional controller and an integral controller, as follows:

$$\delta = \begin{cases} \dfrac{k_i}{s + kk_i}(\omega_0 - \omega), & k(t) > 0 \\ C, & k(t) = 0 \end{cases} \quad (5)$$

being C the last value calculated by the filter just before $k(t) = 0$. Figure 2 presents a scheme of the operation of this proposal. Notice that the value of $k(t)$ controls the transition between modes and affects the cutoff frequency of the low-pass filter. Thus, the time protocol can drive the value of $k(t)$ to obtain the best features of both the filtered proportional controller and the integral controller. This proposal is characterized by a fast speed of response and a good frequency recovery.

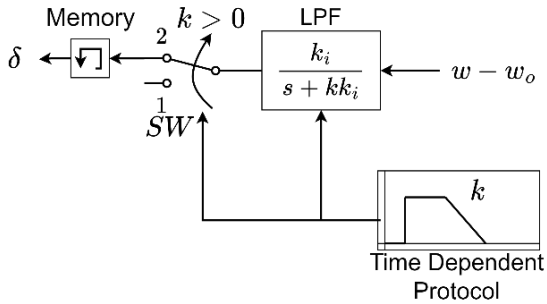

Figure 2. Secondary Switched Control proposed in [20]. Source: elaborated by the authors.

Figure 3 presents the time protocol for variable $k(t)$. This time-protocol is launched when an "event" is detected. According to [20], an "event" is a change in the power delivered or in the frequency of the MG caused by the connection and disconnection of loads and new DGs. Thus, it is possible to implement different approaches for the detection, such as a send-on-delta strategy based on a definition of thresholds for variables such as frequency or active power rate variations [35]. The time protocol is composed of three operation zones: a first operation zone that starts when the event is detected at t_e, in which $k(t)$ has a constant value of k_{max} during a duration of Δ_{ct}. Then, a second operation zone in which $k(t)$ changes in a linear ramp from k_{max} to 0 during Δ_{ramp}, according to equation 5 these operation zones correspond to the filtered proportional controller. Finally, a third operation zone after $t = t_{ramp}$, the switched control maintaining the last value calculated (C in equation 5).

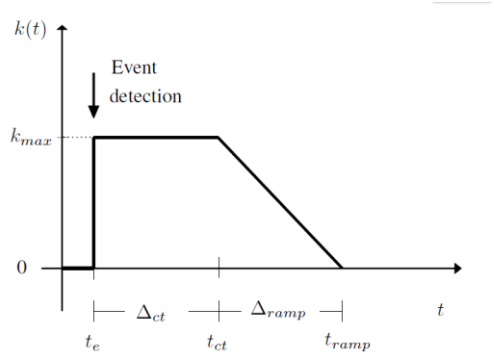

Figure 3. Time protocol for variable k(t) [20].

This strategy was designed to operate on balanced microgrids. However, as will be verified later, the presence of unbalanced loads can lead to problems with the power-sharing performance. For this reason, an additional control block is proposed.

3. Proposed Control Strategy

This section presents the proposed control strategy for the secondary layer of isolated microgrids with unbalanced resistive loads.

3.1. Grid-forming inverter

Figure 4 shows a general scheme of a grid-forming inverter. The DC voltage source presents the DC stage composed of a distributed power source connected through a converter and a DC-link capacitor. At the output of the IGBT power inverter, an LC filter (L_{in}, C) is connected to reduce the high-frequency harmonics [36]. Then, the elements L_T and R_T represent a coupling transformer to connect the inverter to the point of coupling.

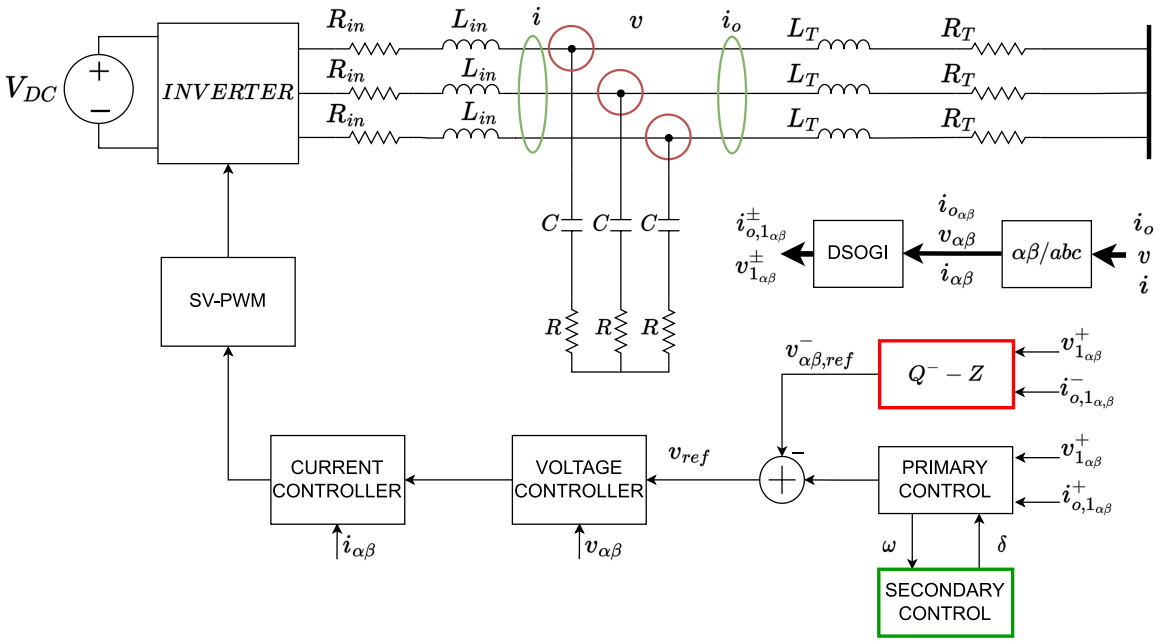

Figure 4. General scheme of a grid-forming inverter. Source: elaborated by the authors.

The sensed signals are $\boldsymbol{i}$, $\boldsymbol{v}$, $\boldsymbol{i_o}$ that correspond to the inverter output current, the voltage at the capacitor of the LC filter and the current injected to the coupling transformer, respectively. These signals are transformed to the αβ framework through the Clarke transformation, and their fundamental positive and negative sequence components are extracted through a double second-order generalized integrator (DSOGI) [37,38].

The fundamental positive sequence components, $v^{+}_{1_{\alpha\beta}}$ and $i^{+}_{o,1_{\alpha\beta}}$, are used for the primary layer block (droop control) and the instantaneous active power p is calculated according to [23] as follows:

$$p^{+} = \frac{3}{2}\left(v^{+}_{1_\alpha} i^{+}_{o,1_\alpha} + v^{+}_{1_\beta} i^{+}_{o,1_\beta}\right) \tag{6}$$

The secondary layer based on the switched control is highlighted in green in Figure 4. It receives the frequency ω and calculates the compensation parameter δ for the primary layer to mitigate the frequency error.

3.2. Proposed control

As previously indicated, the proposed strategy is inspired and adapted from the work presented in [23]. The proposed control corresponds to a $Q^- - Z$ block, which is based on the calculation of a virtual output impedance as a function of the negative reactive power. First, the negative reactive power Q^- is adapted by [23] using $\alpha\beta$ components instead of dq components.

$$Q^- = \frac{3}{2}\sqrt{\left(v^{+}_{1_\alpha}\right)^2 + \left(v^{+}_{1_\beta}\right)^2}\sqrt{\left(i^{-}_{o,1_\alpha}\right)^2 + \left(i^{-}_{o,1_\beta}\right)^2} \tag{7}$$

This reactive power term is used to calculate an output impedance Z using the expression:

$$Z = Z_o + k^{-}(Q^{-} - Q^{-}_{o}) \tag{8}$$

where Z_o, k^- and Q^-_o are an initial output impedance, a proportional negative control coefficient, and an initial negative reactive power, respectively. These parameters can be set to improve the operation of the proposed strategy. Then, the term Z is operated with the negative current $i^-_{o_1}$, as

$$v^{-}_{\alpha\beta,ref} = Z \cdot i^{-}_{o_{1,\alpha\beta}} \tag{9}$$

This $v^{-}_{\alpha\beta,ref}$ signal is applied to the primary control of the hierarchical control structure. The block of the proposed control is highlighted in red in Figure 4.

4. Simulation Results

In order to verify the proposed control strategy, a simulation is implemented in Matlab-Simulink. The simulation was executed on an isolated AC microgrid with the topology presented in Figure 5.

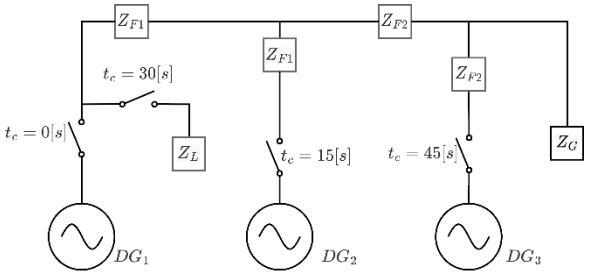

Figure 5. Simulated microgrid. Source: elaborated by the authors.

The grid is composed of three identical inverter-based DGs named DG_1, DG_2 and DG_3, which operate in grid-forming mode. The experimental test reproduces the black start of a microgrid, with the DGs and a local load Z_L being connected sequentially (main load Z_G is connected during all the simulations). DG_1 and DG_2 are connected at $t = 0[s]$ and $t = 15[s]$, respectively. Then, local load Z_L is connected at $t = 30[s]$. Finally, DG_3 is connected at $t = 45[s]$.

The impedances Z_{F1} and Z_{F2} emulate the conductors that connect the equipments and loads. Figure 6 describes the configuration of the loads. The main load Z_G is balanced, as shown in Figure 6(a), while the local load presents an unbalance, as shown in Figure 6(b). It is worth indicating that the load is unbalanced in such a way that the effects on the control strategies were perceptible. The microgrid configuration parameters are described in the table 1.

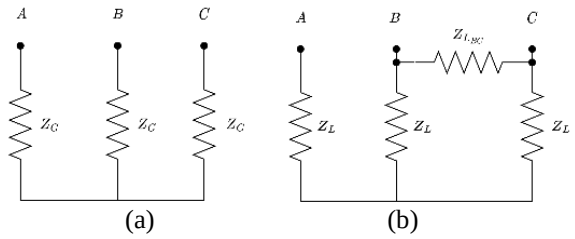

Figure 6. Configuration of the loads: (a) Three-phase global load Z_G. (b) Three-phase local load Z_L. Source: elaborated by the authors.

4.1. Simulation using Only Primary Control Layer

First, the simulation was performed using only the primary control layer. The same value of the droop coefficient *m* was implemented for all the DGs considering converters with equal nominal powers. The results for the instantaneous three-phase active powers and frequencies are presented in figure 7.

Table 1. Microgrid parameters.

Parameter	Symbol	Quantity
Droop coefficient	m	0.5 $rad/(kW.s)$
LC Filter	L_{in},R_{in}, C,R	15 mH, 2.04 Ω, 20 μF, 11.33 Ω
Model coupling transformers	L_T, R_T	1 mH, 0.5 Ω
Feeder impedance	Z_{F1};Z_{F2}	65 $m\Omega$, 2 mH; 110 $m\Omega$, 0.8 mH
Switching frequency	f_{sw}	10 kHz
DC voltage source	V_{DC}	400 V
Local load	Z_L	24.2 Ω
Global load	Z_G	96 Ω
Unbalanced local load	$Z_{L_{BC}}$	72.6 Ω
Initial negative reactive power	Q_o	170 VAr
Initial output impedance	Z_0	4 Ω
Proportional negative control coefficient	k^-	0.01 Ω/VAr
Maximum k gain	k_{max}	0.3
Secondary layer parameter	k_i	90 rad/s
Time interval for constant time	Δ_{ct}	5 s
Time interval for ramp	Δ_{ramp}	5 s

Source: elaborated by the authors.

In these figures, it is possible to clearly observe the effect of the droop method. The primary layer performs fast and accurate power-sharing between the DGs, despite the unbalanced load. However, as previously discussed, the droop characteristic produces a deviation in the frequency. From *t* = 0[s] to *t* = 15[s], when only DG_1 is operating, the frequency presents the greatest deviation because this inverter must deliver all the power demanded. Once the other DGs are connected, the deviation is reduced since the power-sharing is performed.

4.2. Simulation using the Secondary Switched Control

Next, the simulation was performed using the secondary switched control presented in [20]. The results for the instantaneous three-phase active powers and frequencies

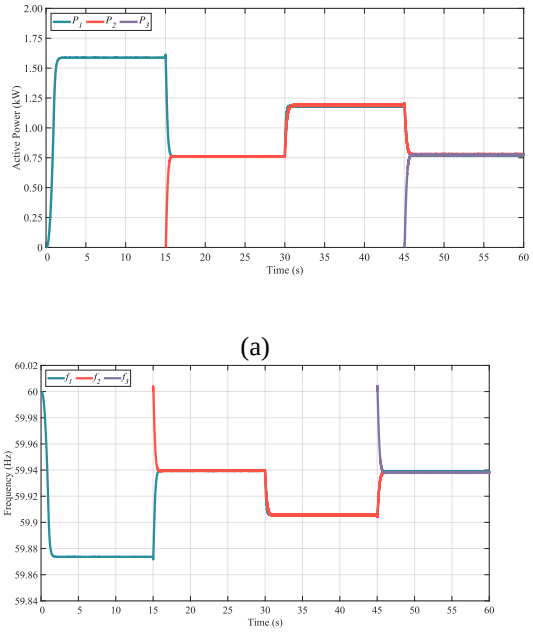

(a)

(b)

Figure 7. Results using only droop method. (a) Instantaneous three-phase active powers for each DG. (b) Frequencies for each DG. Source: elaborated by the authors.

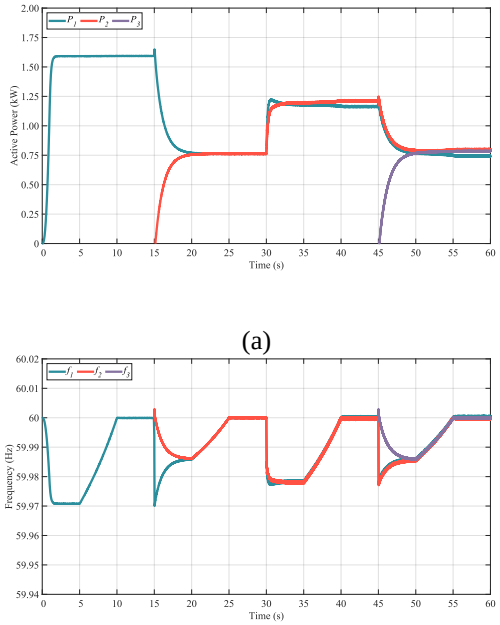

(a)

(b)

Figure 8. Results using secondary switched control. (a) Instantaneous three-phase active powers for each DG. (b) Frequencies for each DG. Source: elaborated by the authors.

are presented in figure 8. The operation of this control strategy requires the detection of "events", which in this case are the connection of the DGs at $t = 0[s]$, $t = 15[s]$ and $t = 45[s]$, and the connection of the unbalanced local load Z_L at $t = 30[s]$.

Since before $t = 30[s]$ the microgrid operates with balanced loads, it is possible to appreciate the proper functioning of the strategy. During the first operation zone that starts when each event is detected (see figure 3), an accurate power-sharing is done during $5[s]$. However, an appreciable error in the frequency recovery can be noted. Next, the parameter $k(t)$ changes in a linear ramp during $5[s]$, compensating for the frequency error and showing a good dynamic response. Finally, once the frequency deviation is eliminated, the control switched maintaining the last value calculated until the next event is detected.

However, despite the good results of the control strategy when the microgrid is balanced, from $t = 30[s]$, once the unbalanced local load Z_L is connected, an error in the steady-state power-sharing is appreciated. Between $40[s]$ and $45[s]$, the difference between the active power delivered by DG_1 and DG_2 is around $50\ [W]$.

Furthermore, between $55[s]$ and $60[s]$, the difference between the active power delivered by DG_1 and DG_2, and DG_1 and DG_3 are around $55[W]$ and $40\ [W]$, respectively. This is because the switched secondary control strategy fails to act over the negative sequence component of the generated powers.

4.3. Simulation using the proposed secondary control layer

Finally, the simulation was performed using the proposed secondary control layer for unbalanced loads. The results for the instantaneous three-phase active powers and frequencies are presented in figure 9. These results allow verifying that the proposed control mitigates the power-sharing error observed in the previous simulation. Thus, with the added control block, it is possible to maintain the performance of the switched control (good dynamic response and frequency restoration in steady state), without being affected by the impact on the negative sequence generated by the operation of unbalanced loads.

5. Conclusions

This paper presented a secondary control strategy to operate in isolated microgrids with unbalanced loads.

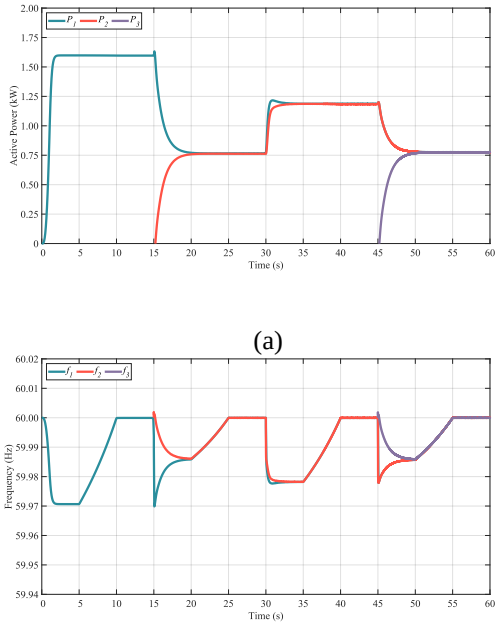

(a)

(b)

Figure 9. Results using unbalanced power-sharing algorithm proposed. (a) Instantaneous three-phase active powers for each DG. (b) Frequencies for each DG. Source: elaborated by the authors.

The proposal does not require the use of communications, as it is based on a communicationless secondary switched control, to which it was adapted a Q-Z control block. This block adds a signal to the primary control, eliminating the mismatch in the power-sharing between DGs through a negative sequence virtual impedance. The selected simulation results show the effectiveness of the proposal in the presence of unbalanced resistive loads.

This work corresponds to the first approximation of the proposed control. Future works will further develop aspects related to the design of the control parameters, stability analysis, and operation in the presence of different unbalanced loads.

Acknowledgments

This work has been supported by UIS and Minciencias, with Project ´´Programa de Investigación en Tecnologías Emergentes para Microrredes Eléctricas Inteligentes con Alta Penetración de energías Renovables´´ contract No. 80740-542-2020.

Conflicts of Interest

The authors declare no conflict of interest.

References

[1] C. Breyer, S. Khalili, D. Bogdanov, M. Ram, A. Solomon-Oyewo, A. Aghahosseini, A. Gulagi, A. A. Solomon, D. Keiner, G. Lopez, P. Østergaard, H. Lund, B. V. Mathiesen, M. Z. Jacobson, M. Victoria, S. Teske, T. Pregger, V. Fthenakis, M. Raugei, H. Holttinen, U. Bardi, A. Hoekstra, B. Sovacool, “On the History and Future of 100% Renewable Energy Systems Research”, *IEEE Access*, vol. 10, pp. 78176-78218, 2022, doi: 10.1109/ACCESS.2022.3193402

[2] M. Farrokhabadi, C. A. Cañizares, J. W. Simpson-Porco, E. Nasr, L. Fan, P. A. Mendoza-Araya, R. Tonkoski, U. Tamrakar, N. Hatziargyriou, D. Lagos, R. W. Wies, M. Paolone, M. Liserre, L. Meegahapola, M. Kabalan, A. H. Hajimiragha, D. Peralta, M. A. Elizondo, K. P. Schneider, F. K. Tuffner, J. Reilly, “Microgrid Stability Definitions, Analysis, and Examples”, *IEEE Transactions on Power Systems*, vol. 35, no. 1, pp. 13-29, 2020, doi: 10.1109/TPWRS.2019.2925703

[3] D. E. Olivares, A. Mehrizi-Sani, A. H. Etemadi, C. A. Cañizares, R. Iravani, M. Kazerani, A. H. Hajimiragha, O. Gomis-Bellmunt, M. Saeedifard, R. Palma-Behnke, G. A. Jiménez-Estévez, N. D. Hatziargyriou, “Trends in Microgrid Control”, *IEEE Transactions on Smart Grid*, vol. 5, no. 4, pp. 1905-1919, 2014, doi: 10.1109/TSG.2013.2295514

[4] M. Aybar-Mejía, J. Villanueva, D. Mariano-Hernández, F. Santos, A. Molina-García, “A Review of Low-Voltage Renewable Microgrids: Generation Forecasting and Demand-Side Management Strategies”, *Electronics*, vol. 10, no. 17, p. 2093, 2021, doi: 10.3390/electronics10172093

[5] J. M. Rey, G. A. Vera, P. Acevedo-Rueda, J. Solano, M. A. Mantilla, J. Llanos, D. Sáez, “A Review of Microgrids in Latin America: Laboratories and Test Systems”, *IEEE Latin America Transactions*, vol. 20, no. 6, pp. 1000-1011, 2022, doi: 10.1109/TLA.2022.9757743

[6] Y. Yoldas ¸, A. ¨Onen, S. Muyeen, A. V. Vasilakos, I. Alan, “Enhancing smart grid with microgrids: Challenges and opportunities”, *Renewable and Sustainable Energy Reviews*, vol. 72, pp. 205–214, 2017, doi: 10.1016/j.rser.2017.01.064

[7] S. Parhizi, H. Lotfi, A. Khodaei, S. Bahramirad, “State of the Art in Research on Microgrids: A Review”, *IEEE Access*, vol. 3, pp. 890-925, 2015, doi: 10.1109/ACCESS.2015.2443119

[8] J. M. Rey-López, P. P. Vergara-Barrios, G. A. Osma-Pinto, G. Ordóñez-Plata, "Generalities about Design and Operation of Microgrids", *DYNA*, vol. 82, no. 192, pp. 109–119, 2015, doi: 10.15446/dyna.v82n192.48586

[9] J. M. Rey, I. Jiménez-Vargas, P. P. Vergara, G. Osma-Pinto, J. Solano, "Sizing of an autonomous microgrid considering droop control", *International Journal of Electrical Power Energy Systems*, vol. 136, p. 107634, 2022, doi: 10.1016/j.ijepes.2021.107634

[10] T. S. Ustun, C. Ozansoy, A. Zayegh, "Recent developments in microgrids and example cases around the world—a review", *Renewable and Sustainable Energy Reviews*, vol. 15, no. 8, pp. 4030–4041, 2011, doi: 10.1016/j.rser.2011.07.033

[11] S. Ansari, A. Chandel, M. Tariq, "A Comprehensive Review on Power Converters Control and Control Strategies of AC/DC Microgrid", *IEEE Access*, vol. 9, pp. 17998-18015, 2021, doi: 10.1109/ACCESS.2020.3020035

[12] J. M. Rey, P. P. Vergara, J. Solano, and G. Ordóñez, "Design and Optimal Sizing of Microgrids", in *Microgrids Design and Implementation*, Cham, Switzerland: Springer Cham, 2019, pp. 337–367.

[13] Y. Khayat, Q. Shafiee, R. Heydari, M. Naderi, T. Dragičević, J. W. Simpson-Porco, F. Dörfler, M. Fathi, F. Blaabjerg, J. M. Guerrero, H. Bevrani, "On the Secondary Control Architectures of AC Microgrids: An Overview", *IEEE Transactions on Power Electronics*, vol. 35, no. 6, pp. 6482-6500, 2020, doi: 10.1109/TPEL.2019.2951694.

[14] S. Liu, X. Wang, P. X. Liu, "Impact of Communication Delays on Secondary Frequency Control in an Islanded Microgrid", *IEEE Transactions on Industrial Electronics*, vol. 62, no. 4, pp. 2021-2031, 2015, doi: 10.1109/TIE.2014.2367456

[15] P. Martí, M. Velasco, E. X. Martín, L. García de Vicuña, J. Miret, M. Castilla, "Performance Evaluation of Secondary Control Policies With Respect to Digital Communications Properties in Inverter-Based Islanded Microgrids", *IEEE Transactions on Smart Grid*, vol. 9, no. 3, pp. 2192-2202, 2018, doi: 10.1109/TSG.2016.2608323

[16] A. K. Sahoo, K. Mahmud, M. Crittenden, J. Ravishankar, S. Padmanaban, F. Blaabjerg, "Communication-Less Primary and Secondary Control in Inverter-Interfaced AC Microgrid: An Overview", *IEEE Journal of Emerging and Selected Topics in Power Electronics*, vol. 9, no. 5, pp. 5164-5182, 2021, doi: 10.1109/JESTPE.2020.2974046

[17] M. Hua, H. Hu, Y. Xing, J. M. Guerrero, "Multilayer Control for Inverters in Parallel Operation Without Intercommunications", *IEEE Transactions on Power Electronics*, vol. 27, no. 8, pp. 3651-3663, 2012, doi: 10.1109/TPEL.2012.2186985

[18] H. Xin, L. Zhang, Z. Wang, D. Gan, K. P. Wong, "Control of Island AC Microgrids Using a Fully Distributed Approach", *IEEE Transactions on Smart Grid*, vol. 6, no. 2, pp. 943-945, 2015, doi: 10.1109/TSG.2014.2378694

[19] H. Xin, R. Zhao, L. Zhang, Z. Wang, K. P. Wong, W. Wei, "A Decentralized Hierarchical Control Structure and Self-Optimizing Control Strategy for F-P Type DGs in Islanded Microgrids", *IEEE Transactions on Smart Grid*, vol. 7, no. 1, pp. 3-5, 2016, doi: 10.1109/TSG.2015.2473096

[20] J. M. Rey, P. Martí, M. Velasco, J. Miret, M. Castilla, "Secondary Switched Control With no Communications for Islanded Microgrids", *IEEE Transactions on Industrial Electronics*, vol. 64, no. 11, pp. 8534-8545, 2017, doi: 10.1109/TIE.2017.2703669

[21] J. M. Rey, C. X. Rosero, M. Velasco, P. Martí, J. Miret, M. Castilla, "Local Frequency Restoration for Droop-Controlled Parallel Inverters in Islanded Microgrids", *IEEE Transactions on Energy Conversion*, vol. 34, no. 3, pp. 1232-1241, 2019, doi: 10.1109/TEC.2018.2886267.

[22] N. Vedaste, N. Emile, Z. Xu, N. Olivier, P. Simiyu, N. Innocent, "Secondary Control for Power Sharing in a Standalone Microgrid under Unequal Feeder Impedance and Complex Loads", in *2018 2nd IEEE Conference on Energy Internet and Energy System Integration (EI2)*, Beijing, 2018, pp. 1-6, doi: 10.1109/EI2.2018.8582271.

[23] Y. Jia, D. Li, Z. Chen, "Unbalanced power sharing for islanded droop-controlled microgrids", *Journal of Power Electronics*, vol. 19, pp. 234–243, 2019, doi: 10.6113/JPE.2019.19.1.234

[24] J. Rey, P. Vergara, M. Castilla, A. Camacho, M. Velasco, P. Martí, "Droop-free hierarchical control strategy for inverter-based ac microgrids", *IET Power Electronics*, vol. 13, no. 7, pp. 1403–1415, 2020, doi: 10.1049/iet-pel.2019.0705

[25] H. Han, X. Hou, J. Yang, J. Wu, M. Su, J. M. Guerrero, "Review of Power Sharing Control Strategies

for Islanding Operation of AC Microgrids", *IEEE Transactions on Smart Grid*, vol. 7, no. 1, pp. 200-215, 2016, doi: 10.1109/TSG.2015.2434849

[26] J. C. Vasquez, J. M. Guerrero, J. Miret, M. Castilla, L. G. de Vicuña, "Hierarchical Control of Intelligent Microgrids", *IEEE Industrial Electronics Magazine*, vol. 4, no. 4, pp. 23-29, 2010, doi: 10.1109/MIE.2010.938720

[27] T. L. Vandoorn, J. C. Vasquez, J. De Kooning, J. M. Guerrero, L. Vandevelde, "Microgrids: Hierarchical Control and an Overview of the Control and Reserve Management Strategies", *IEEE Industrial Electronics Magazine*, vol. 7, no. 4, pp. 42-55, 2013, doi: 10.1109/MIE.2013.2279306

[28] J. M. Guerrero, J. C. Vasquez, J. Matas, L. G. de Vicuna, M. Castilla, "Hierarchical Control of Droop-Controlled AC and DC Microgrids—A General Approach Toward Standardization", *IEEE Transactions on Industrial Electronics*, vol. 58, no. 1, pp. 158-172, 2011, doi: 10.1109/TIE.2010.2066534

[29] J. M. Rey, J. Torres-Martínez, and M. Castilla, "Secondary control for islanded microgrids", in *Microgrids Design and Implementation*, Cham, Switzerland: Springer Cham, 2019, pp. 171–193.

[30] Y. Han, H. Li, P. Shen, E. A. A. Coelho, J. M. Guerrero, "Review of Active and Reactive Power Sharing Strategies in Hierarchical Controlled Microgrids", *IEEE Transactions on Power Electronics*, vol. 32, no. 3, pp. 2427-2451, 2017, doi: 10.1109/TPEL.2016.2569597

[31] P. P. Vergara, J. C. López, J. M. Rey, L. C. P. da Silva, and M. J. Rider, "Energy management in microgrids", in *Microgrids Design and Implementation*, Cham, Switzerland: Springer Cham, 2019, pp. 195–216.

[32] J. M. Rey, J. Solano, J. Torres-Martínez, J. Miret, M. M. Ghahderijani, M. Castilla, "Multi-layer active power and frequency control strategy for industrial microgrids", in *IECON 2017 - 43rd Annual Conference of the IEEE Industrial Electronics Society*, Beijing, 2017, pp. 2588-2593, doi: 10.1109/IECON.2017.8216435

[33] Z. Cheng, J. Duan, M. -Y. Chow, "To Centralize or to Distribute: That Is the Question: A Comparison of Advanced Microgrid Management Systems", *IEEE Industrial Electronics Magazine*, vol. 12, no. 1, pp. 6-24, 2018, doi: 10.1109/MIE.2018.2789926

[34] J. M. Rey, P. P. Vergara, M. Castilla, A. Camacho, J. Miret, "Local hierarchical control for industrial microgrids with improved frequency regulation", in *2018 IEEE International Conference on Industrial Technology (ICIT)*, Lyon, 2018, pp. 1019-1024, doi: 10.1109/ICIT.2018.8352318

[35] B. A. Moser, T. Natschläger, "On Stability of Distance Measures for Event Sequences Induced by Level-Crossing Sampling", *IEEE Transactions on Signal Processing*, vol. 62, no. 8, pp. 1987-1999, 2014, doi: 10.1109/TSP.2014.2305642

[36] U. P. Yagnik, M. D. Solanki, "Comparison of L, LC & LCL filter for grid connected converter", in *2017 International Conference on Trends in Electronics and Informatics (ICEI)*, Tirunelveli, 2017, pp. 455-458, doi: 10.1109/ICOEI.2017.8300968

[37] S. Riyadi, "Inverse Clarke Transformation based control method of a three-phase inverter for PV-Grid systems", in *2014 The 1st International Conference on Information Technology, Computer, and Electrical Engineering*, Semarang, 2014, pp. 351-355, doi: 10.1109/ICITACEE.2014.7065770

[38] A. Milczarek, "Harmonic power sharing between power electronics converters in islanded AC microgrid", in *2017 Progress in Applied Electrical Engineering (PAEE)*, Koscielisko, 2017, pp. 1-7, doi: 10.1109/PAEE.2017.8008991